Available online at www.sciencedirect.com
SCIENCE DIRECT
Journal of Solid State Chemistry 179 (2006) 1129–1135
JOURNAL OF SOLID STATE CHEMISTRY
www.elsevier.com/locate/jssc

Synthesis and adsorption properties of *p*-sulfonated calix[4 and 6]arene-intercalated layered double hydroxides

Satoru Sasaki[a], Sumio Aisawa[a], Hidetoshi Hirahara[a], Akira Sasaki[b], Hirokazu Nakayama[c], Eiichi Narita[a,*]

[a]*Department of Material Science, Graduate School of Engineering, Iwate University, 4-3-5 Ueda, Morioka 020-8551, Japan*
[b]*Department of Sanitary Science, Research Institute for Environmental Sciences and Public Health of Iwate Prefecture, 1-36-1 Iiokashinden, Morioka 020-0852, Japan*
[c]*Department of Functional Molecular Chemistry, Kobe Pharmaceutical University, 4-19-1 Motoyamakitamachi, Higashinada-ku, Kobe 658-8558, Japan*

Received 24 October 2005; received in revised form 29 December 2005; accepted 1 January 2006
Available online 13 February 2006

Abstract

The intercalation of water-soluble *p*-sulfonated calix[4 and 6]arene (CS4 and CS6) in the interlayer of the Mg–Al and Zn–Al layered double hydroxide (LDH) by the coprecipitation method has been investigated, as well as the adsorption properties of the resulting CS/LDHs for benzyl alcohol (BA) and *p*-nitrophenol (NP) to prepare new microporous organic–inorganic hybrid adsorbents. The amount and arrangement of CS intercalated was different by the kind of the host metal ions. CS4 cavity axis was perpendicular for the Mg–Al LDH basal layer and parallel for the Zn–Al LDH basal layer, while CS6 cavity axis was perpendicular for both the LDH basal layers. In the BET surface area measurement, the surface area of the Zn–Al/CS4/LDH was four times than that of the Mg–Al/CS4/LDH, expecting that the former has higher adsorption capacity than the latter. In fact, the adsorption ability of the CS/LDHs for BA and NP in aqueous solution was found to be larger in the Zn–Al/CS4/LDH than in the Mg–Al/CS4/LDH. In addition, the adsorption ability of both the LDHs was larger in the CS6/LDHs than in the CS4/LDHs. These results were explained by the difference in the amount and arrangement of CS intercalated in the LDH interlayer space.

Keywords: Layered double hydroxide; Intercalation; Coprecipitation; Calixarene; Organic–inorganic hybrid materials; Adsorption

1. Introduction

Layered double hydroxide (LDH) is well known as hydrotalcite-like compounds or anionic clay because of its anion exchange property. The chemical composition of LDHs is generally represented as $\left[M^{2+}_{1-x}M^{3+}_{x}(OH)_2\right]^{x+}\left[A^{n-}_{x/n}\cdot yH_2O\right]^{x-}$, where M^{2+} is a divalent cation such as Mg^{2+}, Zn^{2+}, Co^{2+}, Ca^{2+}, Cu^{2+}, etc., M^{3+} a trivalent cation such as Al^{3+}, Cr^{3+}, Fe^{3+}, Co^{3+}, Mn^{3+}, etc., A^{n-} an anion of charge $(n-)$ such as OH^-, Cl^-, NO_3^-, CO_3^{2-}, SO_4^{2-}, etc [1–3]. LDHs consist of positively charged octahedral hydroxide layers and an exchangeable interlayer anion with water molecules [4–6] and are used as versatile material in medical science [7–9], catalysis [10–17], separation technology and nanocomposite materials engineering [18,19].

Since about 20 years ago, much attention has been given to new families of microporous adsorbent resulting from the inorganic layered compounds with polynuclear complex ions or bulky organic molecules [20–22]. LDH is often used as an inorganic host material to synthesize the organic/LDH hybrid material. In addition, the intercalation of the macrocyclic molecules has great attractions [23–27]. As the molecular arrangement in hybrid material can be regulated by nanoscale level, it has the possibility to show the characteristic of not possessing in each organic substance or inorganic substance. Thus, the combination of layered material and intercalation technique will have a possibility of providing new nanohybrid materials [28,29].

Calixarenes are macrocyclic molecules of the metacyclophanes general class, consisting of several phenol units

*Corresponding author. Fax: +81 19 621 6331.
E-mail address: enarita@iwate-u.ac.jp (E. Narita).

0022-4596/$ - see front matter © 2006 Elsevier Inc. All rights reserved.
doi:10.1016/j.jssc.2006.01.012

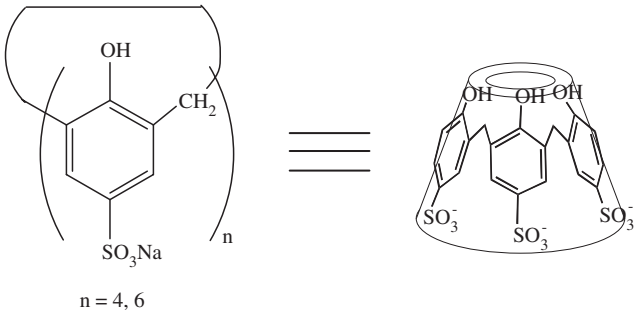

Fig. 1. Structure of the CS.

(usually four to eight) connected via methylene bridges in the ortho position with respect to the hydroxyl group (Fig. 1). It is well established that the cylindral-shaped calixarenes of varying cavity sizes can form a variety of host–guest types of inclusion complexes similar to cyclodextrins. However, calixarene host molecules have a unique composition that includes benzene groups, which provide $\pi-\pi$ interaction, and hydroxyl groups for hydrogen bonding. In 1984, water-soluble calixarenes carrying sulfonate groups have been synthesized [30].

The calixarene cavity is capable of molecular recognition in solution, which is of great interest for application in the remediation of contaminated groundwater and industrial effluents [31–38].

In this study, the intercalation of water-soluble *p*-sulfonated calixarene (CS) in the interlayer of the Mg–Al and Zn–Al LDHs (M^{2+}/Al = 3) by the coprecipitation method has been investigated, as well as the benzyl alcohol (BA) and *p*-nitrophenol (NP) adsorption properties of the resulting CS/LDHs.

2. Experimental

2.1. Materials

Calixarenes and inorganic reagents were purchased from Sugai Chemical Industry Co., Ltd. (Japan) and Wako Pure Chemical Industries, Ltd. (Japan), and used without purification.

2.2. Coprecipitation of calixarenes with the LDH precipitates

The CS/LDHs were prepared by the coprecipitation method under an N_2 atmosphere to avoid contamination by atmospheric CO_2. $M^{2+}(NO_3)_2\cdot 6H_2O$ (M^{2+} = Mg or Zn) (1.5 mmol) and $Al(NO_3)_3\cdot 9H_2O$ (0.5 mmol) were dissolved in distilled water (20 cm^3) and the solution was added dropwise to a solution of CS (1 mmol) in water (100 cm^3) for 1 h. The solution pH was adjusted by dropwise addition of 0.1 mol/dm^3 NaOH solution (pH 10 for Mg–Al, pH 7 for Zn–Al), and the temperature was kept at 40 °C in a thermostat set. The precipitate was separated by centrifugation after aging at 40 °C for 1 h. The supernatant solution was subjected to measurement of the calixarene concentration by using a Shimadzu TOC-5000 total organic carbon (TOC) analyzer. The solid product (precipitate) was washed with distilled water and dried in a vacuum oven at 40 °C for 24 h.

2.3. Characterization of the calixarene/LDHs

Powder X-ray diffraction (XRD) measurements were performed on a Rigaku Rint 2200 powder X-ray diffractometer, using Cu$K\alpha$ radiation (λ = 0.15405 nm) at 20 mA, 40 kV and a scanning rate of 2°/min. Fourier transform infrared (FT-IR) spectra was obtained using a JASCO WS/IR 7300 FT-IR spectrophotometer by the standard KBr disk method. Thermogravimetry (TG) and differential thermal analysis (DTA) were carried out using a Rigaku TG/DTA 320 in the temperature range 25–800 °C in flowing air at a heating rate of 10 °C/min. Chemical analysis date for Al, Mg and Zn were obtained using a Shimadzu AA-6650 atomic absorption spectrophotometer after dissolution of the solid products in 0.1 mol/dm^3 HCl solution. The adsorbates (BA and NP) concentration in the supernatant solution was measured using a Shimadzu TOC-5000 total organic carbon analyzer (TOC) and a JASCO V-570 UV/VIS/NIR spectrophotometer (UV–vis), respectively. Solid-State ^{13}C CP/MAS NMR spectroscopy was performed with a Varian Unity INOVA-500 at 125.7 MHz. The specific surface area was measured by the BET method. The samples were outgased at 100 °C for 2 h. The isotherms using the N_2 adsorption/desorption were measured on a BEL JAPAN BELSORP mini.

2.4. Adsorption properties of the calixarene/LDHs

Adsorption was carried out using the batch method. We adopted BA (p*K*a = 15.4) and NP (p*K*a = 7.15) as the adsorbates, non-anionic and anionic species in the adsorption condition, respectively. The adsorption properties of the CS4/LDHs were estimated by comparing the adsorption results for two organic adsorbates. The CS/LDHs (0.05 g) were added to the aqueous adsorbate solution (10 cm^3) adjusted with pH 10 for Mg–Al and pH 7 for Zn–Al by 0.1 mmol/dm^3 NaOH solution, in which the amount of the adsorbate was two times for CS in the LDH. The suspended mixture was shaken at 25 °C for 24 h using a reciprocating shaker.

3. Results and discussion

3.1. Characterization of the calixarene/LDHs

The chemical compositions of the CS/LDHs are indicated in Table 1. The metal ratio of all the solid products agreed with the mixed ratio (M^{2+}/Al = 3). In the case of the CS4/LDHs, CS4 in the Mg–Al LDH was estimated as $-4\sim-5$ valent species at the synthesis pH. On the other hand, the amount of CS4 intercalated in the

Table 1
Chemical composition of the CS/LDHs

	Chemical formula	M^{2+}/Al	CS/Al[a]
Mg–Al/CS4/LDH	$[Mg_{0.76}Al_{0.24}(OH)_2](CS4)_{0.060}\cdot 0.38H_2O$	3.1	0.25
Zn–Al/CS4/LDH	$[Zn_{0.75}Al_{0.25}(OH)_2](CS4)_{0.030}\cdot 0.70H_2O$	3.0	0.12
Mg–Al/CS6/LDH	$[Mg_{0.75}Al_{0.25}(OH)_2](CS6)_{0.025}\cdot 0.36H_2O$	3.0	0.10
Zn–Al/CS6/LDH	$[Zn_{0.75}Al_{0.25}(OH)_2](CS6)_{0.020}\cdot 0.72H_2O$	3.0	0.08

[a]Theoretical molar ratio of the solid product: $CS4^{4-} = 0.25$, $CS6^{10-} = 0.10$.

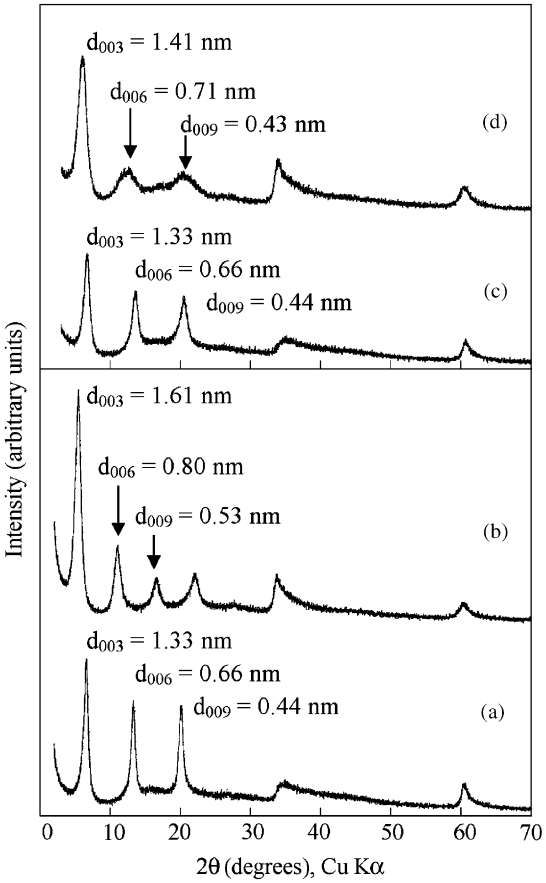

Fig. 2. XRD patterns of the (a) Mg–Al/CS4/LDH, (b) Zn–Al/CS4/LDH, (c) Mg–Al/CS6/LDH, and (d) Zn–Al/CS6/LDH.

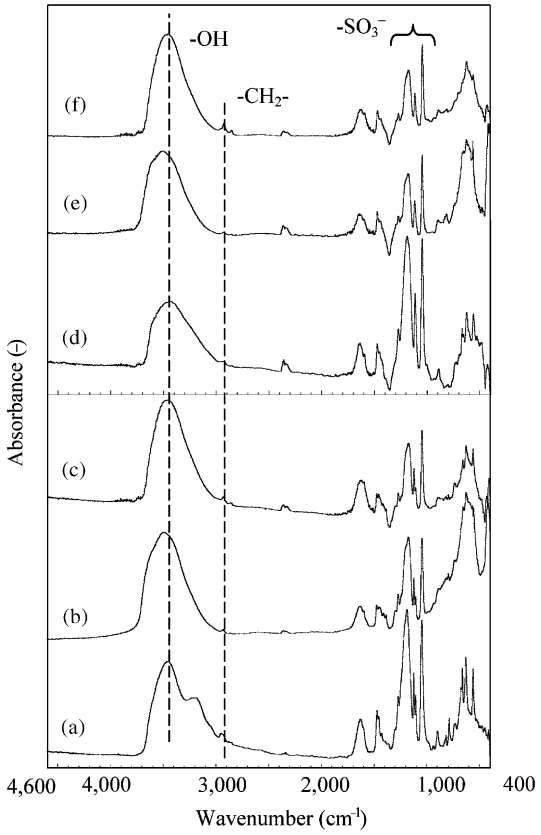

Fig. 3. FT-IR spectra of the (a) CS4, (b) Mg–Al/CS4/LDH, (c) Zn–Al/CS4/LDH, (d) CS6, (e) Mg–Al/CS6/LDH, and (f) Zn–Al/CS6/LDH.

Zn–Al LDH was about one half of that in the Mg–Al LDH. The lower rim combined OH groups in CS4 can be employed to bind with some transition-metal ions and Zn^{2+} ion, but not to bind with Mg^{2+} ion. Since the molecule size of Zn–CS4 complex should be bigger than that of CS4, the amount of CS4 intercalated in the Zn–Al LDH was decreased. In the case of the CS6/LDHs, CS6 in the Mg–Al and Zn–Al LDHs was estimated as −8∼−10 valent species at the synthesis pH.

The XRD patterns of the solid products are shown in Fig. 2. All the solid products were found to have the expanded LDH structure. In the case of the CS4/LDHs shown in Figs. 2a and b, the basal spacing, d_{003}, of the Mg–Al/CS4/LDH was expanded to 1.33 nm, indicating that CS4 anions are a monolayer thickness in the CS4/LDH. Upon considering the original brucite layer thickness of 0.48 nm, CS4 cavity axis was presumed to orient vertically to the LDH basal layer. While for the Zn–Al/CS4/LDH ($d_{003} = 1.61$ nm), CS4 was thought to orient its cavity axis parallel to the LDH basal layer. In the case of the CS6/LDHs shown in Figs. 2c and d, the basal spacings of the Mg–Al and Zn–Al/CS6/LDHs were expanded to 1.33 and 1.41 nm, respectively. CS6 cavity axis was presumed to orient vertically to the LDH basal layer.

The FT-IR spectra of the solid products are shown in Fig. 3. There is no change in CS structure before and after the intercalation. The weak absorption peaks of methylene bridges –CH_2– were observed in the region 2915–2940 cm^{-1} and the strong absorption peaks of S–O were observed in the region 1037–1040 cm^{-1}. A broad absorption peak in the

region 3000–3600 cm^{-1} is assigned to OH group stretches of both hydroxides for the basal layer and the interlayer CS molecule.

The Raman spectra of the solid products are presented in Fig. 4. The weak absorption peaks of methylene bridges $\nu(CH_2)$ were observed in the region 2878–2950 cm^{-1} and the strong absorption peaks of $\nu(SO_3^-)$ were observed in the region 1045–1128 cm^{-1}. Each absorption peak of the CS/LDHs moved on the side of lower wavenumber than that of the naked CS. Therefore, CS in the interlayer of LDH was ionized as sulfonate and had electrical interaction with the positively changed basal layer.

Fig. 5 shows the ^{13}C CP/MAS NMR spectra of the solid products. The shift of C1(C–O) and C2(C–S) peaks to the lower frequency regions was recognized. It suggests that the interaction of the intercalated CS with the host hydroxide layers was generated. Moreover, the resonance of the cointercalated CO_3^{2-} was observed at 180.2 ppm.

Fig. 6 shows the schematic representation of structure models of the CS/LDHs. The CS4/LDHs have two types of micropores, i.e. the CS4 cavity and intermolecular space. We considered two reasons for such difference in CS4 conformation. First, the arrangement of CS4 in the interlayer space of the LDHs was presumed to be different by the number of dissociated OH group ($pKa_1 = 3.08$, $pKa_{2-4} > 11$) [39], namely, the strength of the electrostatic force of attraction between the negative CS4 and the positive LDH basal layer. The synthesis pH of the Mg–Al/CS4/LDH (pH 10) was higher than that of the Zn–Al/CS4/LDH (pH 7). Therefore, CS4 molecule takes a perpendicular monolayered arrangement within the Mg–Al/LDH interlayers as show in Fig. 6a. Second reason, the formation of Zn–CS4 complexes would obstruct the interaction between the dissociated OH groups of CS4 and the LDH basal layer. Therefore, CS4 was considered to orient its cavity axis parallel to the Zn–Al LDH basal layer as shown in Fig. 6b. Similarly, the arrangement of CS6 in the interlayer space of the LDHs was presumed to be different by the number of dissociated OH group ($pKa_1 = 3.45$, $pKa_2 = 5.02$, $pKa_{3-6} > 11$) [39]. As the molecular size of CS6 was larger than that of CS4, CS6 conformation was same direction within the Mg–Al and Zn–Al LDH. In addition, the synthesis pH of the Zn–Al/CS6/LDH (pH 7) causes conformation change of CS6, double partial cone conformation [40]. Therefore, CS6 molecules take a perpendicular monolayered arrangement within the Zn–Al LDH interlayers as show in Fig. 6d.

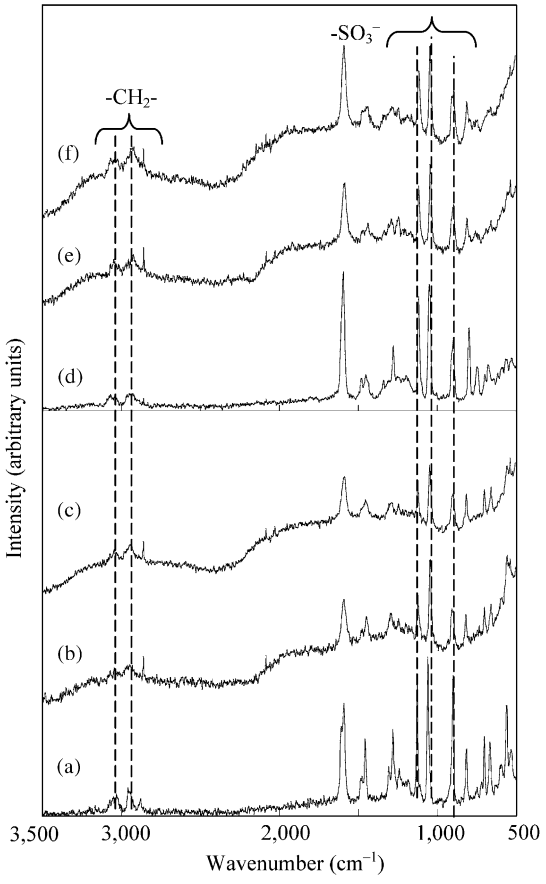

Fig. 4. Raman spectra of the (a) CS4, (b) Mg–Al/CS4/LDH, (c) Zn–Al/CS4/LDH, (d) CS6, (e) Mg–Al/CS6/LDH, and (f) Zn–Al/CS6/LDH.

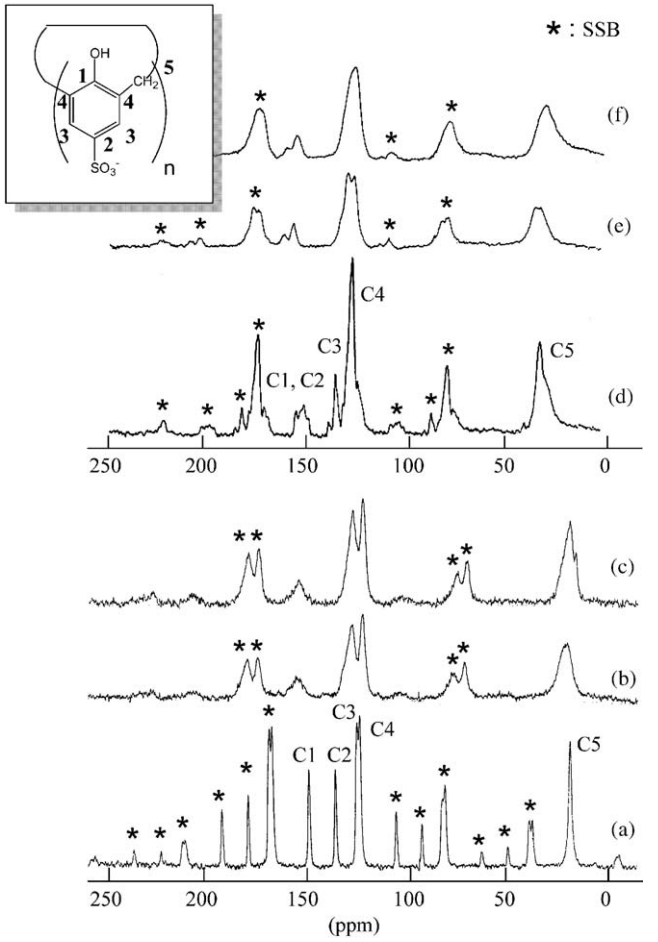

Fig. 5. ^{13}C CP/MAS NMR spectra of (a) CS4, (b) Mg–Al/CS4/LDH, (c) Zn–Al/CS4/LDH, (d) CS6, (e) Mg–Al/CS6/LDH, and (f) Zn–Al/CS6/LDH.

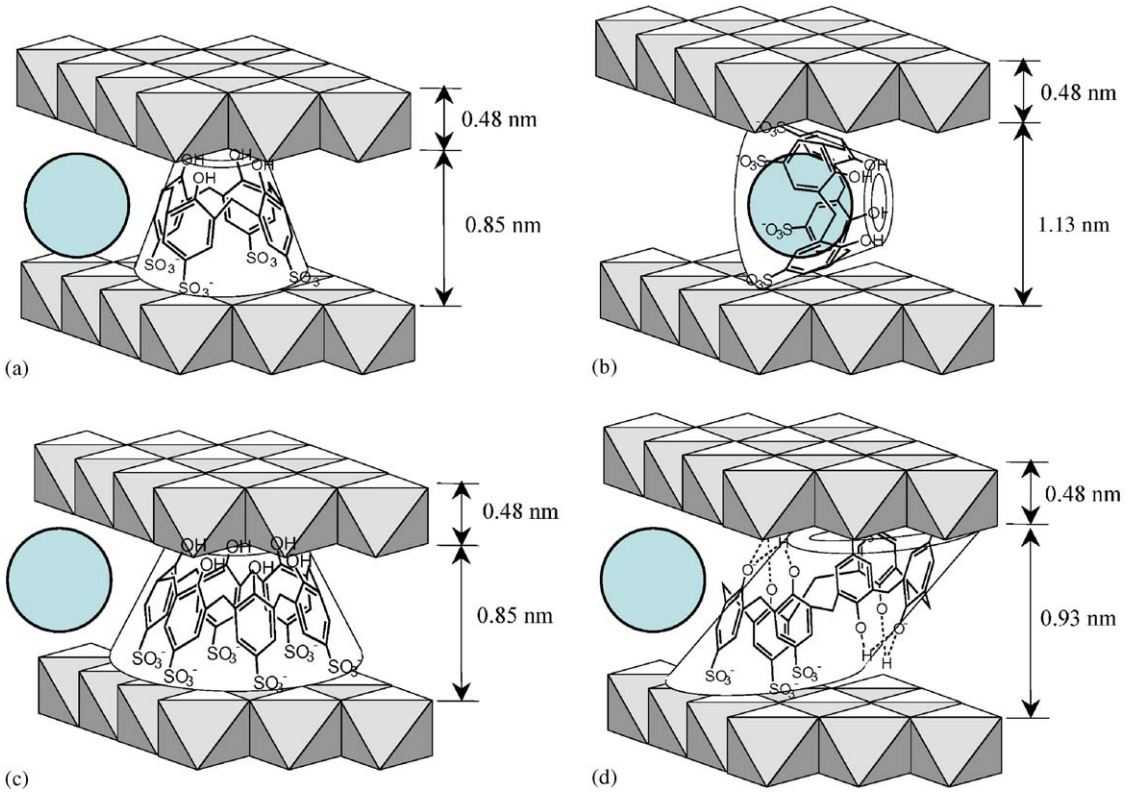

Fig. 6. Schematic representation of CS oriented in interlayer space of LDH. (a) Mg–Al/CS4/LDH (pH 10, $CS4^{5-}$), (b) Zn–Al/CS4/LDH (pH 7, $CS4^{5-}$), (c) Mg–Al/CS6/LDH (pH 10, $CS6^{10-}$), and (d) Zn–Al/CS6/LDH (pH 7, $CS6^{8-}$).

3.2. Adsorption properties of the calixarene/LDH

The BET surface area and N_2 adsorbed volume of the CS/LDHs are indicated in Table 2 and the adsorption–desorption curves of the CS/LDHs are also displayed in Fig. 7. The features of all the CS/LDHs can be classified as the intermediate type between types II and IV. This result indicates that the CS/LDHs have a mesopore along with micropore. Fig. 8 shows the pore size distribution of the CS/LDHs in which a sharp and high peak around 2.0 nm appears in all the desorption curves. Entirely, the pore size distribution curve was broad and ranged to a micropore side. The N_2 adsorbed volume was found to be greater for the Zn–Al/CS4/LDH than for the Mg–Al/CS4/LDH. The result can be explained by the difference in CS4 arrangement in the interlayer space of the LDH. In the BET surface area measurement, the surface area of the Zn–Al/CS4/LDH was four times that of the Mg–Al/CS4/LDH, expecting that the Zn–Al/CS4/LDH has higher adsorption capacity than that of the Mg–Al/CS4/LDH. As a reference, the same measurement was carried out using the NO_3/LDHs, and no difference between the Mg–Al and Zn–Al LDHs was observed.

Compositional data for the CS/LDHs obtained after the adsorption in aqueous solutions are also indicated in Table 3. In the adsorption experiments, the CS/LDHs were found to adsorb BA and NP in each aqueous solution with keeping the LDH structure. The basal spacing of the CS/LDHs and the amount of CS in the CS/LDHs were not

Table 2
BET surface area and absorbed volume for the CS/LDHs

	S_{BET} ($m^2\,g^{-1}$)	Adsorbed volume ($mm^3\,g^{-1}$)
Mg–Al/CS4/LDH	22.4	49.6
Zn–Al/CS4/LDH	79.0	161
Mg–Al/CS6/LDH	41.7	121
Zn–Al/CS6/LDH	94.5	285
Mg–Al/NO_3/LDH	8.95	29.7
Zn–Al/NO_3/LDH	8.17	30.1

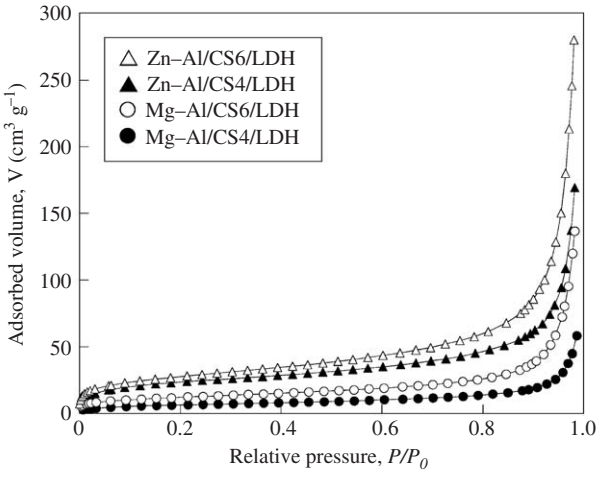

Fig. 7. N_2 adsorption isotherm for the CS/LDHs.

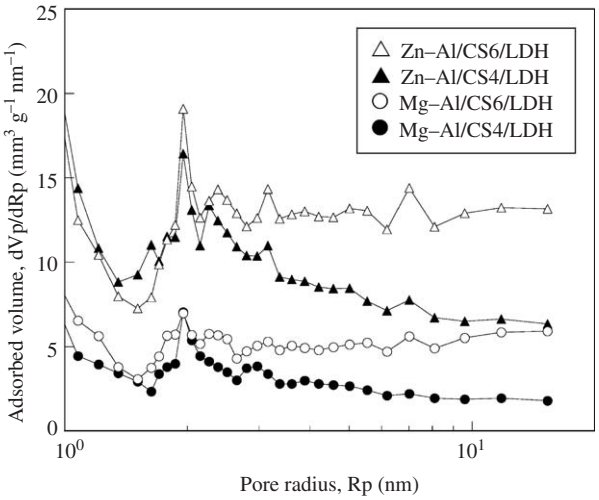

Fig. 8. Pore size distributions of desorption side for the CS/LDHs.

Table 3
Adsorption properties data for the CS/LDHs

	Molar ratio of the solid products		
	CS/Al	BA/CS	NP/CS
Mg–Al/CS4/LDH	0.25	0.22	0.76
Zn–Al/CS4/LDH	0.12	2.10	4.50
Mg–Al/CS6/LDH	0.10	2.60	4.40
Zn–Al/CS4/LDH	0.08	6.10	8.60

changed before and after the adsorption. For each adsorbate, the adsorption ability of the Zn–Al/CS4/LDH was much greater than that of the Mg–Al/CS4/LDH. In addition, the adsorption ability of both the LDHs was larger in the CS6/LDHs than in the CS4/LDHs. This result was similar to the N_2 gas adsorption data.

The adsorption of BA by the Zn–Al/CS4/LDH was considered to relate not only to the interlayer space but also to the intercalated calixarene cavity. As no adsorption of BA for the LDHs incorporating inorganic guest anions was observed in the preliminary experiments, the driving force of BA adsorption was thought to be based on the presence of CS4 in the LDH interlayer. In the adsorption of NP, the CS4/LDHs indicated the same tendency. In addition, the adsorbed amount of NP was higher than that of BA because NP can be attracted not only by CS4 but also by the LDH basal layer. The results suggest that the CS4/LDHs can adsorb non-anionic and anionic organo molecules. Strict interaction between CS4 molecule and organic adsorbates in the LDH interlayer is as yet unclear.

4. Conclusions

The investigation has led to a new finding for the intercalation of water-soluble macrocyclic molecules, CS4 and CS6, in the interlayer of LDHs. Some of the important findings of this study can be summarized as follows. (I) The Mg–Al and Zn–Al/CS/LDHs were synthesized by the coprecipitation method. (II) The amount and arrangement of CS4 was different by the kind of the host metal ions, as CS4 cavity axis perpendicular (Mg–Al LDH) and parallel (Zn–Al LDH) to the basal layer. (III) The BET surface area and N_2 gas adsorbed pore volume were larger in the Zn–Al/CS/LDH than in the Mg–Al/CS/LDH. (IV) The adsorption ability for BA and NP in aqueous solution are also larger in the Zn–Al/CS4/LDH than in the Mg–Al/CS4/LDH because of effective use of the parallel-arranged CS4 cavity only in the Zn–Al/CS4/LDH. (V) The CS/LDHs have a considerable possibility as new organic–inorganic hybrid adsorbents for many organic molecules.

Acknowledgment

The authors are grateful to Mr. S. Takahashi (Iwate University) for his helpful assistance in the instrumental analyses.

References

[1] R. Allman, Chimia 24 (1970) 99–108.
[2] H.F.W. Taylor, Miner. Mag. 39 (1973) 377–389.
[3] S. Miyata, T. Kumura, Chem. Lett. (1973) 843–848.
[4] S. Aisawa, S. Takahashi, W. Ogasawara, Y. Umetsu, E. Narita, J. Solid State Chem. 162 (2001) 52–62.
[5] S. Aisawa, H. Hirahara, K. Ishiyama, W. Ogasawara, Y. Umetsu, E. Narita, J. Solid State Chem. 174 (2003) 342–348.
[6] S. Aisawa, H. Kudo, T. Hoshi, S. Takahashi, H. Hirahara, Y. Umetsu, E. Narita, J. Solid State Chem. 177 (2004) 3987–3994.
[7] J.-H. Choy, J.-S. Jung, J.-M. Oh, M. Park, J. Jeong, Y.-K. Kang, O.-J. Han, Biomaterials 25 (2004) 3059–3064.
[8] S.-Y. Kwak, W.M. Kriven, M.A. Wallig, J.-H. Choy, Biomaterials 25 (2004) 5995–6001.
[9] B. Li, J. He, D.G. Evans, X. Duan, Int. J. Pharm. 287 (2004) 89–95.
[10] T.J. Pinnavaia, M. Chibwe, V.R.L. Constantino, S.K. Yun, Appl. Clay Sci. 10 (1995) 117–129.
[11] M.C. Hermosin, I. Pavlovic, M.A. Ulibarri, J. Cornejo, Water Res. 30 (1996) 171–177.
[12] J.J. Alcaraz, B.J. Arena, R.D. Gillespie, J.S. Holmgren, Catal. Today 43 (1998) 89–99.
[13] M. Lakraimi, A. Legrouri, A. Barroug, A. de Roy, J.-P. Besse, J. Chem. Phys. 96 (1999) 470–478.
[14] Y. Guo, D. Li, C. Hu, Y. Wang, E. Wang, Y. Zhou, S. Feng, Appl. Catal. B: Environ. 30 (2001) 337–349.
[15] V.R. Choudhary, S.K. Jana, A.B. Mandale, Catal. Lett. 74 (2001) 91–94.
[16] B.M. Choudary, M.L. Kantam, V. Neeraja, K.K. Rao, F. Figueras, L. Delmotte, Green Chem. 3 (2001) 257–260.
[17] E.M. Serwicka, Pol. J. Chem. 75 (2001) 307–328.
[18] V. Rives, M.A. Ulibarri, Coord. Chem. Rev. 181 (1999) 61–120.
[19] A.I. Khan, D. O'Hare, J. Mater. Chem. 12 (2002) 3191–3198.
[20] T. Kijima, J. Tanaka, M. Goto, Nature 310 (1984) 45–47.
[21] T. Kijima, Y. Matsui, Nature 322 (1986) 533–534.
[22] T. Kijinma, Y. Kato, K. Ohe, M. Machida, Y. Matsushita, T. Matsui, Bull. Chem. Soc. Jpn. 67 (1994) 2125–2129.
[23] H. Zhao, G.F. Vance, J. Chem. Soc. Dalton Trans. (1997) 1961–1965.
[24] H. Zhao, G.F. Vance, Clays Clay Miner. 46 (1998) 712–718.
[25] H. Zhao, G.F. Vance, J. Inclusion Phenom. 31 (1998) 305–317.
[26] R. Sasai, D. Sugiyama, S. Takahashi, Z. Tong, T. Shichi, H. Itoh, K. Tkagi, J. Photochem. Photobiol. A. 155 (2003) 223–229.
[27] J. Wang, M. Wei, G. Rao, D.G. Evans, X. Duan, J. Solid State Chem. 177 (2004) 366–371.

[28] S. Sasaki, S. Aisawa, H. Hirahara, A. Sasaki, E. Narita, Chem. Lett. 33 (2004) 790–791.
[29] S. Sasaki, Y. Yokohama, S. Aisawa, H. Hirahara, E. Narita, Chem. Lett. 34 (2005) 1192–1193.
[30] S. Shinkai, S. Mori, T. Tsubaki, T. Sone, O. Manabe, Tetrahedron Lett. 25 (1984) 5315–5318.
[31] S. Shinkai, S. Mori, H. Koreishi, T. Tsubaki, O. Manabe, J. Am. Chem. Soc. 108 (1986) 2409–2416.
[32] S. Shinkai, K. Araki, T. Matsuda, N. Nishiyama, H. Ikeda, I. Takasu, M. Iwamoto, J. Am. Chem. Soc. 112 (1990) 9053–9058.
[33] I. Yoshida, N. Yamamoto, F. Sagara, K. Ueno, D. Ishii, S. Shinkai, Chem. Lett. (1991) 2105–2108.
[34] J.L. Awood, D.L. Clark, R.K. Juneja, G.W. Orr, K.D. Robinson, R.L. Vincent, J. Am. Chem. Soc. 114 (1992) 7558–7559.
[35] J.-P. Scharff, M. Mahjoubi, New. J. Chem. 17 (1993) 793–796.
[36] N. Douteau.-Guével, A.W. Coleman, J.-P. Morel, N. Morel-Desrosiers, J. Chem. Soc. Perkin Trans. 2 (1999) 629–633.
[37] G. Arena, A. Contino, F. Giuseppe Gulino, A. Magri, D. Sciotto, R. Ungaro, Tetrahedron Lett. 41 (2000) 9327–9330.
[38] C. Bonal, Y. Israëli, J.-P. Morel, N. Morel-Desrosiers, J. Chem. Soc. Perkin Trans. 2 (2001) 1075–1078.
[39] J.-P. Scharff, M. Mahjoubi, New J. Chem. 15 (1991) 883–887.
[40] J. Alvarez, Y. Wang, W. Ong, A.E. Kaifer, J. Supra. Chem. 1 (2001) 269–274.